

# SYNTHESIS AND SPECTRA OF A GROUP OF HYDROXY FERRIC SULFATES RELEVANT TO MARS.

Hongkun Qu<sup>1,2</sup>, Alian Wang<sup>2</sup>, and Zongcheng Ling<sup>1</sup>, <sup>1</sup>Shandong Key Laboratory of Optical Astronomy and Solar-Terrestrial Environment, School of Space Science and Physics, Institute of Space Sciences, Shandong University, Weihai, Shandong, 264209, China. ([quhongkun@mail.sdu.edu.cn](mailto:quhongkun@mail.sdu.edu.cn)). <sup>2</sup>Dept. of Earth and Planetary Sciences and the McDonnell Center for the Space Sciences, Washington University in St. Louis, One Brookings Drive, St. Louis, MO, 63130, USA ([alianw@levee.wustl.edu](mailto:alianw@levee.wustl.edu)).

**Introduction:** Mars carries a name of “Red Planet” because of its reddish appearance. The surficial color of Mars has been attributed to ferric-bearing phase in the regolith that was supported by mission observations[1]. Ferric sulfates have been found on Mars by observations of orbiters, lander, and rovers. The *Opportunity* rover revealed the existence of Jarosite [ $\text{KFe}^{3+}(\text{SO}_4)_2(\text{OH})_6$ ] in outcrops at Meridiani Planum (over hundreds kilometers) using Mössbauer spectroscopy[2]. Ferric hydroxy-sulfate [ $\text{Fe}(\text{SO}_4)\text{OH}$ ] was suggested existing in the sedimentary deposits in Aram Chaos[3] using VNIR spectroscopy. The *Spirit* rover identified different kinds of ferric sulfates within the subsurface regolith at Gusev crater[8, 9]. A VNIR spectral analysis using Pancam data of subsurface materials, excavated by the *Spirit* rover in Gusev crater at three different locations, implied the presence of a mixture of basic, neutral, and acidic ferric sulfates with various degrees of hydration, including ferricopiapite [ $\text{Fe}^{2+}_{2/3}\text{Fe}^{3+}_4(\text{SO}_4)_6(\text{OH})_2 \cdot 20(\text{H}_2\text{O})$ ], hydronium jarosite [ $(\text{H}_3\text{O})\text{Fe}^{3+}_3(\text{SO}_4)_2(\text{OH})_6$ ], fibroferrite [ $\text{Fe}^{3+}(\text{SO}_4)(\text{OH}) \cdot 5(\text{H}_2\text{O})$ ], rhomboclase [ $\text{HFe}^{3+}(\text{SO}_4)_2 \cdot 4(\text{H}_2\text{O})$ ] and paracoquimbite [ $\text{Fe}^{3+}_2(\text{SO}_4) \cdot 9(\text{H}_2\text{O})$ ] [10]. It is nevertheless hard to make definitive identification of these hydrated ferric sulfates due to the heavily overlapped VNIR spectral bands, as well as the lacking of laboratory spectral studies of a wide variety of hydrated ferric sulfates. More importantly, yellowish soil at Tyrone site in Gusev crater has shown a Pancam spectral changes after being exposed to current Martian surface atmosphere for 175 sols, determined to be caused by the dehydration of hydrous ferric sulfates[11]. This finding demonstrated not only the huge different environmental conditions at surface and within the subsurface of Mars, but also the needing of knowledge on the pathway of phase transition among ferric sulfates.

The difficulty in these mission data interpretations calls for a deeper understanding of fundamental properties of ferric sulfates. Up to now, eight hydrous ferric sulfates [12], four mixed cation

ferric sulfates [13], and a set of Na, K,  $\text{H}_3\text{O}$ -jarosite solid solutions [14, 15] have been synthesized in laboratory, and their spectral characteristics studied. This study reports our effort to synthesize the hydroxy ferric sulfates in fibroferrite-group,  $\text{Fe}(\text{SO}_4)(\text{OH}) \cdot x\text{H}_2\text{O}$  ( $x=0, 2, 5$ ), and the spectral characterizations.

**Synthesis of Ferric Hydroxy Sulfates:** We chose melanterite, a mineral form of hydrous iron(II) sulfate  $\text{FeSO}_4 \cdot 7\text{H}_2\text{O}$ , as the starting phase for the synthesis. 20 g melanterite was grinded with an agate mortar, then was held by a crucible with a cap.  $\text{Fe}(\text{SO}_4)\text{OH}$  is synthesized by heating this sample at 240 °C for 24hrs in a muffle furnace. In order to synthesize butlerite  $\text{Fe}(\text{SO}_4)(\text{OH}) \cdot 2\text{H}_2\text{O}$  and fibroferrite  $\text{Fe}(\text{SO}_4)(\text{OH}) \cdot 5\text{H}_2\text{O}$ , Relative Humidity (RH) buffer solutions were employed for  $\text{Fe}(\text{SO}_4)\text{OH}$  to rehydrate under controlled temperature (T) and RH. The LiBr, LiCl,  $\text{MgCl}_2$ ,  $\text{Mg}(\text{NO}_3)_2$ , NaBr, KI, NaCl, KCl,  $\text{KNO}_3$  saturated aqueous solutions and pure water can provide 6-100% RH between 5 and 80 °C [14, 16, 17]. We found that butlerite  $\text{Fe}(\text{SO}_4)(\text{OH}) \cdot 2\text{H}_2\text{O}$  can be synthesized in a RH range of 30-80% between 5 and 80 °C. It would take 15 days to form butlerite when the small bottle which contained  $\text{Fe}(\text{SO}_4)\text{OH}$  sample was held in NaCl saturated aqueous solution at 80 °C. Up to now, we synthesized two salts in fibroferrite-group,  $\text{Fe}(\text{SO}_4)\text{OH}$  and butlerite, successfully. Then we employed Raman, MIR and VNIR spectroscopic methods to study their spectral characteristics related to crystal structures.

**Molecular Spectral Characterizations:** As shown in Fig.1, In the principal  $\text{H}_2\text{O}/\text{OH}$  Raman spectral region,  $\text{Fe}(\text{SO}_4)\text{OH}$  has a single narrow peak at  $3452\text{ cm}^{-1}$ . Butlerite has two wide overlapped peaks ( $3453$  and  $3294\text{ cm}^{-1}$ ) contributed by its structural  $\text{H}_2\text{O}$ .  $\text{SO}_4$  usually

shows four fundamental vibrational modes.  $\nu_1$  symmetric and  $\nu_3$  antisymmetric stretching modes occur  $> 900\text{ cm}^{-1}$ .  $\nu_2$  symmetric and  $\nu_4$  antisymmetric bending modes occur around  $400$  and  $600\text{ cm}^{-1}$ . The  $\nu_1$  mode was observed at  $1098\text{ cm}^{-1}$

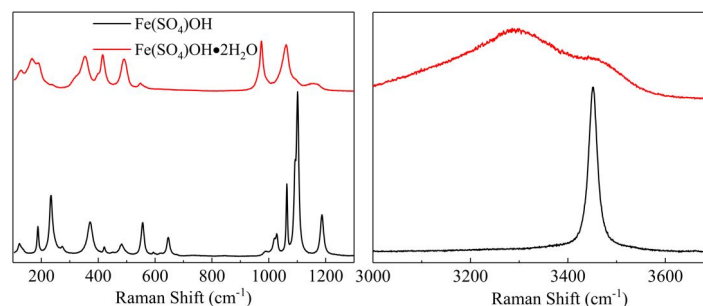
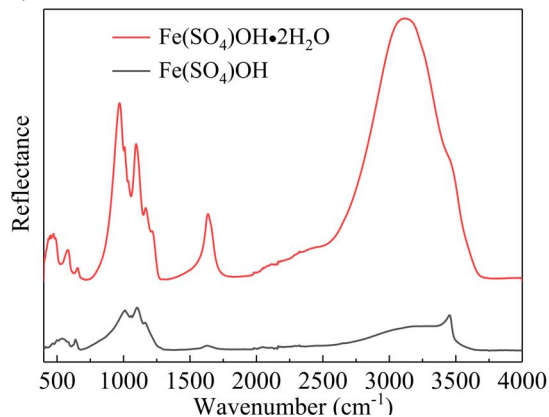


Fig. 1 Raman spectra of  $\text{Fe}(\text{SO}_4)\text{OH}$  and butlerite

in the spectrum of  $\text{Fe}(\text{SO}_4)\text{OH}$  and  $1024\text{ cm}^{-1}$  in butlerite, with  $\nu_3$  modes at  $1186$ ,  $1101$ , and  $1062\text{ cm}^{-1}$  for  $\text{Fe}(\text{SO}_4)\text{OH}$ , and at  $1109$  and  $1224\text{ cm}^{-1}$  for butlerite. Raman peaks of butlerite at  $405$  and  $468\text{ cm}^{-1}$ , and shoulders at  $373$  and  $450\text{ cm}^{-1}$  are assigned to  $\nu_2(\text{SO}_4)^{2-}$  symmetric bending vibrations [18]. The  $645\text{ cm}^{-1}$  peak in  $\text{Fe}(\text{SO}_4)\text{OH}$  and  $601$  and  $542\text{ cm}^{-1}$  in butlerite are assigned to their  $\nu_4(\text{SO}_4)^{2-}$  asymmetric bending mode. Raman peaks appeared between  $300$  and  $150\text{ cm}^{-1}$  are assigned to the Fe-O and Fe-OH stretching and lattice vibration modes, e.g.,  $186$  and  $232\text{ cm}^{-1}$  in  $\text{Fe}(\text{SO}_4)\text{OH}$  and  $184$ ,  $221$  and  $242\text{ cm}^{-1}$  in butlerite.



**Fig. 2 Infrared spectra of  $\text{Fe}(\text{SO}_4)\text{OH}$  and butlerite**

The strong and wide Mid-IR band ( $3126\text{ cm}^{-1}$ ) and shoulder ( $3455\text{ cm}^{-1}$ ) of butlerite in  $\text{H}_2\text{O}/\text{OH}$  spectral region were assigned to the vibrations of its structural  $\text{H}_2\text{O}$  molecules [18].  $\text{Fe}(\text{SO}_4)\text{OH}$  has a narrow single OH peak ( $3455\text{ cm}^{-1}$ ), connected to a broad shoulder due to the absorbed  $\text{H}_2\text{O}$  in the sample. Butlerite has a strong  $\text{H}_2\text{O}$  bending mode at  $1636\text{ cm}^{-1}$ .  $\nu_3(\text{SO}_4)^{2-}$  (triple degenerated) band consists five sub-peaks at  $1035$ ,  $1097$ ,  $1124$ , and  $1218\text{ cm}^{-1}$  in butlerite, and  $1054$ ,  $1100$ , and  $1164\text{ cm}^{-1}$  in  $\text{Fe}(\text{SO}_4)\text{OH}$ . The  $\nu_1(\text{SO}_4)^{2-}$  feature occurs at  $1005$  and  $969\text{ cm}^{-1}$  in  $\text{Fe}(\text{SO}_4)\text{OH}$  and in butlerite respectively. The  $\nu_4(\text{SO}_4)^{2-}$  mode could be seen at  $652$  and  $579\text{ cm}^{-1}$  in butlerite and  $636\text{ cm}^{-1}$  in  $\text{Fe}(\text{SO}_4)\text{OH}$ .

The VNIR spectra of  $\text{Fe}(\text{SO}_4)\text{OH}$  and butlerite [ $\text{Fe}(\text{SO}_4)\text{OH}\cdot 2\text{H}_2\text{O}$ ] are normally contributed by overtones, combinational modes of  $\text{H}_2\text{O}$  & OH groups, and the Metal-OH stretching (Fig. 3). For  $\text{Fe}(\text{SO}_4)\text{OH}$ , the absorptions at  $1489$ ,  $1833$ ,  $2237$ , and  $2384\text{ nm}$  are very narrow, matching well with the narrow OH fundamental stretching mode seen in Raman and MIR spectra ( $3452\text{ cm}^{-1}$ ). The spectral band centered at  $428$  and  $954\text{ nm}$  are attributed to  $\text{Fe}^{3+}$  electronic transitions [20]. For butlerite, the feature at  $2241\text{ nm}$  is assigned to OH combination stretching plus bending vibration mode. The  $\text{H}_2\text{O}$  stretching overtone and combination band of butlerite are at  $1476$  and  $1502\text{ nm}$ , and at  $1960$  and  $2026\text{ nm}$  [20].

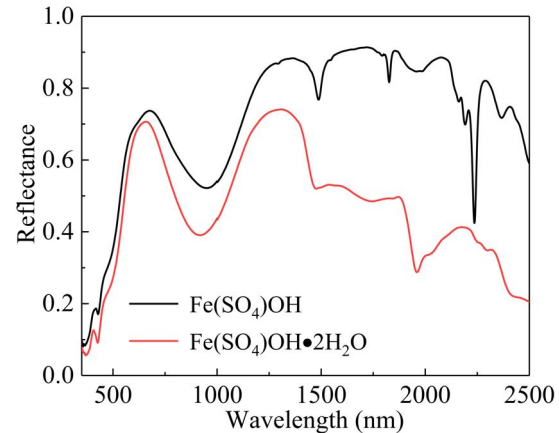


**Fig. 3 VNIR spectra of  $\text{Fe}(\text{SO}_4)\text{OH}$  and butlerite**

**Further work:** We are going to keep working on the synthesis of fibroferrite-group and to characterize them with Raman, Mid-IR and VNIR. The investigations on the phase transformation pathways of fibroferrite-group will provide some assistance for interpreting the future Mars mission observations

#### Acknowledgments:

This work was supported by the CSC scholarship (NO. 201906220244) for HKQ to support his joint-training PhD study at Washington University in St. Louis; and by a special funding 94351A of WUSTL\_MCSS to AW to maintain a collaboration with planetary scientists and students from Shandong University in China.

**References:** [1] Burns et al., (1987) *JGR: Solid Earth*, 92, E570-E574. [2] Klingelhofer et al., (2004) *Science*, 306, 1740-1745. [3] Lichtenberg et al., (2010) *JGR*, 115, E6. [4] Vaniman et al., (2006) *AM*, 91, 1628-1642. [5] Wang et al., (2009) *LPSC*. [6] Tosca et al., (2004) *JGR: Planet*, 109, E5. [7] McLennan et al., (2007) *LPI Contributions*, 1353, 3231. [8] Klingelhofer et al., (2004) *Science*, 306, 1740-1745. [9] Morris et al., (2006) *JGR: Planet*, 111, E2. [10] Johnson et al., (2007) *GRL*, 34, L13202. [11] Wang et al., (2008) *JGR*, 113, E12. [12] Ling & Wang, (2010) *Icarus*, 209, 422-433. [13] Kong et al., *JRS*, (2011); [14] Ling et al., (2010) *Icarus*, 209, 422-433; [15] Cao et al., (2016) *JRS*; [16] Chou et al., (2002) *AM*, 87, 108-114. [17] Greenspan et al., (1997) *Journal of research of the National Bureau of Standards. Physics and chemistry*, 81, 89-96. [18] Jiri Cejka et al., (2011), *Spectrochimica Acta Part A*, 79, 1356-1363. [19] Sasak et al., (1998), *The Canadian Mineralogist*, 36, 1225-1235. [20] Lichtenberg et al., (2010), *JGR*, 115, E00D17.